

## Agent-based modelling of wind damage processes and patterns in forests

Kana Kamimura<sup>a,\*</sup>, Barry Gardiner<sup>b,c</sup>, Sylvain Dupont<sup>b</sup>, John Finnigan<sup>d</sup><sup>a</sup> School of Science and Technology, Shinshu University, 8304 Minamiminowa, Nagano, Japan<sup>b</sup> ISPA, INRA, Bordeaux Sciences Agro, Villenave d'Ornon, France<sup>c</sup> European Forest Institute Planted Forests Facility, 69 Route d'Arcachon, 33612, Cestas, France<sup>d</sup> CSIRO Oceans and Atmospheres, Synergy Building, CSIRO Black Mountain Science and Innovation Park, Acton, ACT, 2600, Australia

## ARTICLE INFO

## Keywords:

Wind damage  
Agent-based model  
Forest edge  
Damage propagation  
Damage pattern  
Gust

## ABSTRACT

Powerful storms, consisting of strong gusts and winds, damage forests. Therefore, foresters need forest management strategies to reduce the damage risk. This paper focused on the damage patterns within the forest as the final results of multiple tree-wind dynamic interactions in time and space during a storm. Recent developments in computer technology allow for the possibility of simulating the complex and dynamic phenomena of damage during a storm but are extremely time consuming. To simplify the simulations without losing the crucial aspects of wind damage in forests, we introduced a computer simulation model using the agent-based modelling (ABM) technique, which capture the phenomena and interactions of individuals called 'agents'. We created an ABM for forest wind damage simulation, coupling together an accepted understanding of wind gusts in forests, tree bending moments, and damage propagation. The model was tested with variations in three conditions: trees acclimated and unacclimated to their wind environment; three levels of gust strength; and three tree planting densities. The ABM was able to replicate damage patterns and demonstrate damage propagation within the forest and the effects of forest edges. The difference in the rate of damage in the forest between acclimated and unacclimated edges became similar with an increase in the gust intensity, and a decrease in tree density through a reduction in the shelter effect of the forest. The ABM could be improved in the future by parametrizing the variation in individual tree resistance, and the variation in gust and wind strength, as well as adding more information on local environmental conditions such as topography and soil variation, and storm characteristics such as duration and intensity.

## 1. Introduction

Powerful storms, consisting of strong gusts and winds, cause enormous damage to forests (e.g. Cucchi and Bert, 2003; Mitchell, 2013; Gardiner et al., 2016) due to the accumulated temporal and spatial interactions between trees and the wind during a storm. Fig. 1 shows three examples of damage: (A) almost all trees are blown down except at the forest edge; (B) damage is only found in the lee of the forest edge; (C) damaged trees are along stream-wise lines. These different patterns are evidence of the various dynamic processes and mechanisms occurring in forests during storms. However, we cannot directly observe what is happening to forests during storms due to the difficulty of data collection, the need to predict damaging storms in advance, safety concerns for personnel entering forests during storms, and current technologies (e.g. satellites and drones) being unable to record the damage dynamics during storms.

The interaction between trees, wind, and environmental conditions

makes direct observations difficult (Gardiner et al., 2016) and also tree damage propagates with time, increasing the overall levels of damage (Dupont et al., 2015). Therefore, previous research has focussed on only a few factors linked to damage occurrence. The airflow behaviour above or within a canopy and the characteristics and properties of the trees and forest are associated with different degrees of damage (e.g., Schmidt et al., 2010). The forest edge (a distance of ~5 to 8 tree heights back from the edge) is a key in understanding forest damage because coherent gusts, intensifying with an increase in distance from the forest edge, lead to mechanical damage to trees (Gardiner, 1994, 1995; Dupont and Brunet, 2009). In addition, the outer-wood dynamic modulus of elasticity and tree height increase (Brüchert and Gardiner, 2006; Bascuñán et al., 2006) and there are changes in tree bending moment (Gardiner et al., 1997) with distance from the forest edge. Forest edges and the distance from the forest edge thus help to explain the different damage spatial patterns recognized in Fig. 1. However, they still cannot explain why the level of damage and the damage

\* Corresponding author at: School of Science and Technology, Shinshu University, 8304 Minamiminowa, Kamiina, Nagano, 399-4598, Japan.

E-mail address: [kamimura@shinshu-u.ac.jp](mailto:kamimura@shinshu-u.ac.jp) (K. Kamimura).

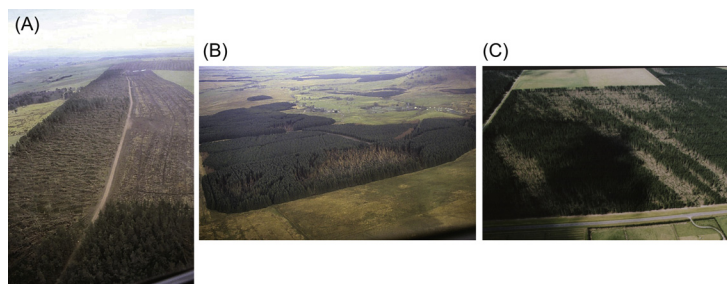


Fig. 1. Wind damage patterns observed after storms; (A) and (B) are Sitka spruce in north-west England, and (C) radiata pine in New Zealand. Photos (A) and (B) were taken by Graeme Prest, Forest Enterprise Scotland (used with permission) and (C) by John Moore, Scion (used with permission).

patterns differ and how the damage changes with time and space during a storm. To do that an alternative modelling approach is required with a focus on the changing interaction between the wind and the trees with time and space.

Seidl et al. (2014) analysed the dynamics of forest damage using a landscape computer simulation model presenting the effects of gap size and local shelter from neighbouring trees, but tree acclimation to the wind environment and damage propagation were absent. Byrne and Mitchell (2013) demonstrated forest damage propagation during storms by integrating wind damage, growth, and wind simulation models. It helps decision making in forest management, yet it disregarded the actual mechanism of damage occurrence. Dupont et al. (2015) used a more direct approach to simulate damage propagation in forests using a large eddy simulation, which could capture the temporal and spatial interactions between trees and wind gusts. They focused on the inside of an infinite artificial forest with a single failure type, stem breakage, and thus it is impossible to investigate the effects of the forest edge from their simulations. Also for forest management, we need to simulate wind damage with different forest conditions due to tree growth and management, but with mechanistic or numerical models it is difficult to test many different settings because these models require long simulation times and an enormous effort to set up different model parameters and environments (Dupont et al., 2015). To consider forest management for reducing wind damage risk, we need to use alternative modelling approaches to obtain both the dynamic behaviours of tree and airflow and interactions between key factors with various environmental and forest settings.

In this paper, we apply a simulation method, known as Agent-based modelling (ABM), which represents the behaviour of individual agents (independent components in a model) under the influence of their environment (Grimm et al., 2006; Railsback and Grimm, 2010; Wilensky

and Rand, 2015). One of the strongest advantages of ABM is the ability to integrate many different levels or fields in the environment, such as agent behaviour and ecosystem ecology using a set of simplified assumptions (Huston et al., 1988). As a result, ABM allows simulations of complicated phenomena without being too time-consuming. For this reason, we assumed that ABM would be a possible candidate to analyse the interactions of trees, wind, and forest conditions including management activities. One drawback of ABM is its dependence on the user model settings without a standard protocol with equations and rules (Grimm et al., 2006). Therefore, the procedures to control individual agent behaviour need to be carefully addressed in this paper.

We aimed to develop a prototype ABM for wind damage at stand-level using knowledge about wind gusts, tree bending moment, and damage propagation, and to show how the dynamic processes captured in the ABM result in realistic damage patterns (e.g., those illustrated in Fig. 1). We simulated wind damage with tree acclimation and lack of acclimation to their wind environment, three gust intensity levels, and different inter tree spacing. The absence of dynamic damage data during storms makes it difficult to fully validate the ABM; nevertheless, this paper is a first attempt at understanding the damage processes and patterns in forests by focusing on the dynamic interactions between wind and trees. We hope that the ABM approach can contribute to developing new forest damage estimation methods in the future.

## 2. Methods

To develop an ABM for wind damage, we had to create two model components: agents and their environment. An agent is an independent entity with certain characteristics and actions, and the environment is where the agents operate. Interacting with the other agents and the environment, the agents exhibit both temporal changes of behaviour

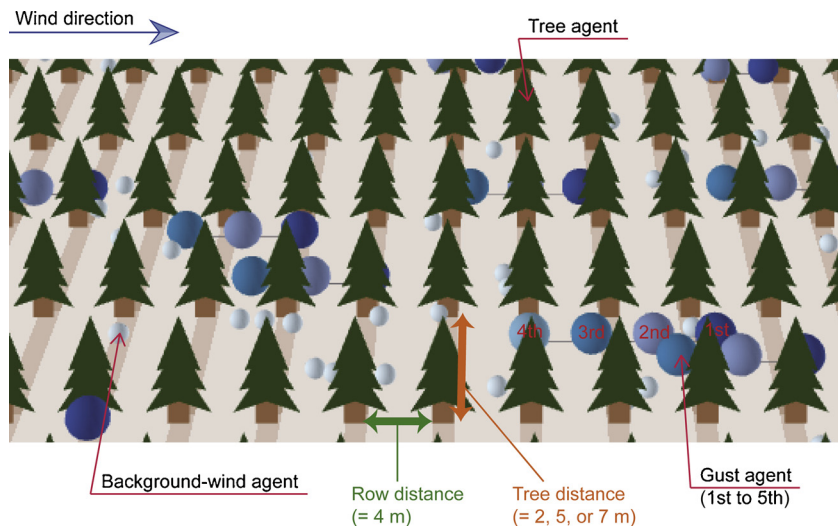


Fig. 2. Three agents; tree, gust (large blue balls), and background-wind (small light-blue balls) and the tree and row spacing settings for the forest damage ABM. The gust and background-wind agents sometimes hit the tree agents as part of their movement (For interpretation of the references to colour in this figure legend, the reader is referred to the web version of this article).

and operating rules (Wilensky and Rand, 2015). Fig. 2 shows the model components: tree, gust, and background-wind within the simulation setting. Large coherent gust structures are created over forests when an instability is produced in the mean velocity profile by the arrival from above of boundary layer scale gusts that produce much higher velocities above the canopy than the local mean velocity. This instability produces oscillations in the flow and leads to well-defined vortices embedded in the mean flow (Raupach et al., 1996; Finnigan et al., 2009). Hence, we configured two kinds of airflow agents: forest gust and background-wind, which produced damage impacts on the tree agents. The following sections present the detailed configurations. Our model was two-dimensional in order to minimize simulation time; therefore, vertical conditions, such as tree height and gust and wind vertical structure, were not incorporated in the model except for the values of tree height being used as a length scale in the horizontal direction. We used the software NetLogo version 5.3.1 by Uri Wilensky (<https://ccl.northwestern.edu/netlogo/>) to create the prototype ABM and the simulations.

### 2.1. Environment (forest) configurations

The simulation environment was described by grid cells, each representing  $10^{-4}$  ha ( $1\text{ m} \times 1\text{ m}$ ). The simulated forests were maritime pine (*Pinus pinaster* Aiton) even-aged forests typical of the Nouvelle-Aquitaine region, south-west France. The model trees were assigned an initial resistance against gust and wind pressure (explained in the following sections). The modelled forest area was 3 ha (100 m from north to south and 300 m from west to east, totalling 30,000 grid cells) with a 1.1 ha upwind open area (100 m from north to south and 110 m from west to east). The wind and gust always came from the west, which is similar to the prevailing wind in the region. The edge of the model forest was on the west side facing the wind direction with a length of 100 m.

Maritime pine trees in the region are normally planted in lines separated by 4 m with a spacing between trees of approximately 2 m. The planting lines faced the prevailing wind direction in the model. We simulated the model with tree densities from an original planting and two systematic thinnings, giving three tree densities:  $4\text{ m} \times 2\text{ m}$  (1250 tree/ha),  $4\text{ m} \times 5\text{ m}$  (500 tree/ha), and  $4\text{ m} \times 7\text{ m}$  (360 trees/ha).

### 2.2. Agent configurations

All agents were defined by values denoting either tree resistance against gusts and background-winds (i.e., degree of fatigue of a tree due to pressure from gusts and background-winds) or the strength of gusts and the background-winds (see also Fig. 2). Table 1 defines the agent configurations and behaviours and responses. We also present the fundamental properties of each agent as a function of distance from the

forest edge in Fig. 3, based on the following understanding:

- 1 Tree: The resistance of the trees to being damaged depends on acclimation due to the level of shelter from neighbouring trees (Gardiner et al., 2016), so that trees at the forest edge are more resistant because they have been subjected to higher wind loading during growth. This is reflected in the acclimated agent behaviour (green solid line in Fig. 3).
- 2 Gust: Intense gusts at canopy level result from the ‘mixing layer instability’ process (Raupach et al., 1996; Finnigan et al., 2009) triggered by strong wind events developed higher in the planetary boundary layer (PBL) and extending over hundreds of tree spacings. It takes some distance behind the forest edge before the developing ‘mixing layer inflected velocity profile’ becomes deep enough to generate damaging gusts (Belcher et al., 2012). This is reflected in the gust strength gradient downwind of the edge illustrated by the blue line in Fig. 3.
- 3 Background-wind: The mean wind speed in the PBL close to the surface during a storm (defined as background-wind) decays downwind of the forest edge as an internal boundary layer of slower air speeds develops over the canopy (Garratt, 1990). This is reflected in the exponential decay of the background-wind agent illustrated by the orange line in Fig. 3.

#### 2.2.1. Gust agent

Gust agents occur in groups consisting of 1–5 individuals (Finnigan and Shaw, 2000) and the number of gust agents within a group is positively skewed following Dupont (2016), which shows the distribution of the normalized wind velocity component parallel to the mean wind direction had a long tail and an extremely high peak in maritime pine forests. To simplify the calculation, our model used a Poisson distribution of gusts with mean = 2, which gave the highest frequency to a gust group with 1- and 2-individuals and the lowest frequency to a gust group with 5-individuals. We also calculated the spatial density of gust agents for the simulations. Kaimal and Finnigan (1994) defined the peak streamwise eddy wavelength ( $\lambda_u$ ) at canopy top in terms of the canopy height ( $h$ ) such that  $\lambda_u \approx 6.5h$  (see their Fig. 3.13). With a tree height of 20 m, the wavelength was approximately 100–200 m, which is equal to 100–200 grids in the model. The total number of the forest grids was 30,000, so the model should have 150–300 gust agents over the forest. We used 300 gust agents and based on a Poisson distribution the number of gust agent groups was approximately 130 in the simulations (see Table 1).

The gust agents only emerged over the forest (grids including tree agents) through a pseudo-random method, calculated using date and time in the simulation computer. Stronger gusts appear at a distance of a few tree heights back from the forest edge because this distance is required for them to fully develop (Finnigan and Brunet, 1995; Dupont

**Table 1**

Initial configurations of the AMB model and functions of the three agents; gust, background-wind, and tree during a simulation.

Categories	Agent		
	Gust	Background-wind	Tree
<b>Configuration</b>			
Total number of agents <sup>a</sup>	300	1100	1125-3825
Key energy values	Strength	Strength	Resistance
Formation	Groups of 1-5 individuals	Individuals	Individuals
Frequency of groups	Poisson distribution	None	None
Function from the forest edge	Logistic	Exponential	Constant for unacclimated; Exponential for acclimated
Location of appearance	Pseudo-random	Pseudo-random	Fixed
<b>Behaviour/Response</b>			
Movement	West to East (left to right)	West to East (left to right)	None
Interaction	Tree	Tree	Gust, background-wind; Neighbouring tree conditions
Disappearance	After moving 35-45 m	After moving 35-45 m	When the resistance = 0

<sup>a</sup> The numbers changed during a simulation.

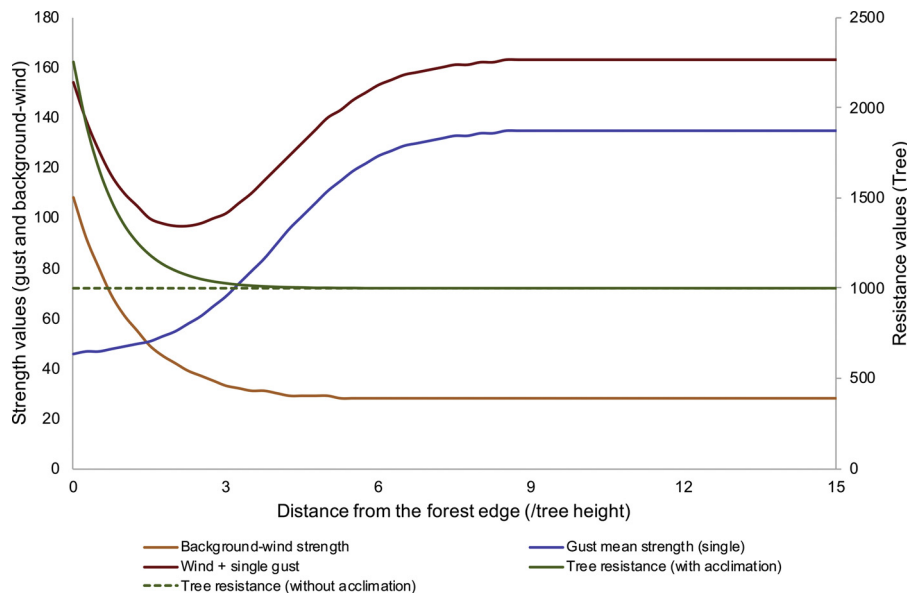


Fig. 3. Model configurations of gust, background-wind, and the initial resistance of tree against gust and background-wind with distance from the forest edge. Overall gust strength is the total value of a group (1 to 5 gust agents). 0 m is denoted as the forest edge and  $h$  is tree height (20 m in the simulation).

and Brunet, 2009; Belcher et al., 2012). The ratio of the maximum to the mean bending moment on trees (gust factor), which follows a logistic relationship with distance from the forest edge (Gardiner et al., 2005), is also related to gust development downwind of the forest edge (Dupont and Brunet, 2009). Hence, we used the measured pattern of gust factor, being low at the forest edge and increasing with distance from the edge, to represent the gust strength ( $G_s$ , unit-less). The initial strength of the gust agents replicated this pattern and it gradually decreased by one measurement unit with every move downwind over a distance of 35 to 45 grids (explained in 2.3.1). The minimum initial strength of the gust agent,  $G_{s-min}$ , was a value of 45 to avoid negative values. Using the pattern in Fig. 6 of Gardiner et al. (2005) with this minimum value, the maximum strength  $G_{s-max}$  was 136 (value well back from the edge). Mean  $G_s$  ( $G_{s-mean}$ ) of a single gust was then computed using the following expression,

$$G_{s-mean} = (G_{s-max} - G_{s-min}) / (1 + \exp[-(x - c)/h]) + G_{s-min} \quad (1)$$

where  $x$  is the distance from the forest edge (m),  $c$  is the centre of the logistic model, which was  $4 \times \text{tree height} = 80$  m in this model, and  $h$  is tree height (m).  $G_s$  varied based on a normal distribution containing 95% of representations within 2 standard deviations, i.e. mean =  $G_{s-mean}$ , and standard deviation = 9 for the simulations. The distance  $x$  is the distance from the solid edge, so at each point in the forest  $x$  reduced during the simulation as damage occurred at the edge. When the number of surviving trees was less than 10% of the original number of trees between the edge and  $n \times \text{tree heights}$  inside the edge, the edge moved downwind  $n \times \text{tree heights}$  (where  $n = 1, 2, \text{ or } 3$  and tree height = 20 m in this paper). Different intensities of  $G_s$ : 50, 100, and 200% of the normal gust strength were also examined to analyse how the overall gust strength relative to the background-wind (see below) impacted on damage levels in the model forest.

### 2.2.2. Background-wind agents

While coherent tree-height scale gusts are located only above the canopy, strong winds can be observed anywhere during a storm. In this paper, we called such winds background-wind agents, pseudo-randomly appearing at any position in the simulation boundary, even outside the forest. Eq. (4) in Gardiner et al. (2000) gives the mean bending moment ( $BM_{mean}$ ) on a tree as a function of the ratio of distance from the forest edge to tree height:

$$BM_{mean} = (0.68D/h - 0.0385) + (-0.68D/h + 0.478) \cdot (1.7239D/h + 0.0316)^{x/h} \quad (2)$$

where  $D$  (m) is tree spacing. We assumed  $BM_{mean}$  could also represent the average wind force on trees and used to calculate the background-wind agent strength values,  $W_s$  (unit-less). The background-wind agents reduced the resistance of tree agents when they interacted with them.  $W_s$  was calculated using  $BM_{mean}$ , the minimum wind strength value inside the forest ( $W_{s-min}$ ), and an adjustment factor ( $F_{forest-mean}$ ) to ensure  $W_s$  has the value  $W_{s-min}$  at the back of the model forest,

$$W_s = BM_{mean} \cdot W_{s-min} / F_{forest-mean} \quad (3)$$

where  $F_{forest-mean}$  was obtained by replacing  $x$  in Eq. (2) with the maximum distance downwind of the edge in the simulation forest, which was 300 m.  $W_{s-min}$  was calculated from  $G_{s-max}$  (= 136) divided by the gust factor ( $GF$ ) at the back of the forest ( $GF = BM_{max} / BM_{min} = \text{Eq. (4)} / \text{Eq. (2)}$  with  $x$  set to 300 m).

The background-agent could emerge anywhere in the simulation boundary ( $410 \times 100$  grid cells), and the number of winds directly reducing the tree resistance was assumed to be in the upper part of a normal distribution (above 2 standard deviations of the mean = 2.5%), so the number of background-wind agents was 1025 ( $41,000 \times 0.25$ ). In the simulations we used 1100 background-wind agents.

### 2.2.3. Tree agents

The tree agents were given a resistance value against the gusts and background-winds. The value decreased when an interaction occurred with a gust or background-wind agent (i.e. tree and gust or background-wind agents situated at the same grid cell) or the upwind trees were damaged. The decrease in resistance describes the gradual fatiguing of the trees leading to a higher possibility of damage. The method of reducing the values is explained in section 2.3.3. For the acclimated setting, the values were calculated using a modified version of the equation of  $BM_{max}$  with distance from the forest edge (Eq. (5) in Gardiner et al., 2000):

$$BM_{max} = 2.7193D/h - 0.061 + (-1.273D/h + 0.9701) \cdot (1.1127D/h + 0.0311)^{x/h} \quad (4)$$

$BM_{max}$  was then transformed to the model value ( $TR$ ) describing the degree of tree resistance against gusts and background-winds. This simulation used a tree resistance value 1000, exceeding the maximum

**Table 2**

18 scenario names for the forest damage simulations based on tree distance, consisted of A (acclimated to the wind environment) or N (not acclimated), tree spacing: 2, 5, and 7 m, and the gust intensity: 50, 100, and 200%.

Tree spacing: 2m	Tree spacing: 5m	Tree spacing: 7 m
A-2m-50%	A-5m-50%	A-7 m-50%
A-2m-100%	A-5m-100%	A-7 m-100%
A-2m-200%	A-5m-200%	A-7 m-200%
N-2m-50%	N-5m-50%	N-7 m-50%
N-2m-100%	N-5m-100%	N-7 m-100%
N-2m-200%	N-5m-200%	N-7 m-200%

mean gust strength values ( $136 \times 5$ ), as the constant tree resistance for the unacclimated setting and as the minimum value for the acclimated setting.  $TR$  was calculated as follows:

$$TR = BM_{max} \cdot TR_{min} / F_{forest-max} \quad (5)$$

where  $TR_{min}$  is the minimum tree resistance value (1000) and  $F_{forest-max}$  is again an adjustment factor (to ensure  $TR$  equals  $TR_{min}$  at the back of the model forest), which was calculated using Eq. (4) by replacing  $x$  with the maximum distance in the simulation, which was 300 m.

### 2.3. Agent behaviour and response

#### 2.3.1. Gust agents

Three main assumptions were applied to the gust agents. First, they moved one grid cell every time step in one direction, from the west to the east (the left to right side of the simulation area), and lost one strength value for every movement. Second, the agents disappeared after some distance. The shear stress from the large eddies influences gusts (Finnigan and Shaw, 2000), which disappear at a distance dependent on the plant canopy. In the model, the distance over which the gust agents exist was assumed to be equal to the eddy wavelength where the vertical wind spectra peaks ( $\approx 2 \times$  tree height: Fig. 3.13 in Kaimal and Finnigan, 1994) because the vertical penetration of a gust into the canopy damages the trees. Therefore, the gust agents disappeared randomly after moving between 35 to 45 m, which was simply determined by  $2 \times$  tree height (40 m) with a variation of  $\pm 5$  m. Third, the 1st gust agents were always created first and then the 2nd to 5th agents attached to the spatially-nearest gust agent, i.e. the 2nd gust agent always attached to the 1st agent, the 3rd attached to the 2nd, and so on (see Fig. 2). When the 1st gust agent vanished, the attached agents also disappeared at the same time. Therefore, the length of the gust agent group depended on the number of agents in a group and this created different levels of impacts on trees along the same stream-wise direction. The total number of gust agents was almost constant during a simulation period by reproducing new gusts as existing gusts disappeared. The gust agents emerged only in the grid cells with a tree agent and inside of the forest edge, thus the total number of agents slowly decreased with the simulation time as the size of the forest reduced due to damage.

#### 2.3.2. Background-wind agents

The movement of background-wind agents was similar to that of the gust agents (moving one grid cell every time step in one direction and disappearing after moving from 35 to 45 cells) except they were always independent and able to be placed anywhere, even outside the forest. Thus, the total number of the background-agents was always the same during a simulation.

#### 2.3.3. Tree agents

When the gust or background-wind agents encountered a tree agent, the tree resistance value was reduced by the value of the gust or background-wind agent. When the tree resistance was zero (negative values were treated as zero), the trees disappeared from the simulation

environment (treated as damaged) following a binary rule: damaged or not damaged. The damaged trees influence the downwind trees (Dupont et al., 2015) and, because gap size is associated with changes in maximum wind loading on trees, Eq. (9) in Peltola et al. (1999) was used to adjust tree resistance as a function of the size of any upwind gap:

- 1) no upwind trees for  $1 \times$  tree height reduced the tree resistance to 60%,
- 2) no upwind trees for  $5 \times$  tree height reduces the resistance to 45%, and
- 3) no upwind trees for  $10 \times$  tree height reduces the resistance to 33%. To shorten the simulation time, we designed a cone-shaped sector with an angle of  $10^\circ$  instead of a square, using the in-cone function in NetLogo. In the unacclimated setting, the trees at the edge (similar to after an upwind clear felling) were assumed to have reduced resistance against the wind because of having no neighbouring trees for shelter, so
- 4) the edge trees had a reduced resistance of 33% at the first step of the simulation (like example 3 above).

### 2.4. Simulation

We tested how the new model represented typical damage as illustrated in Fig. 1 using settings of a tree spacing of  $4 \text{ m} \times 5 \text{ m}$  and 100% gust intensity. 18 scenarios were examined with three different tree spacings (2, 5, and 7 m), edge trees either acclimated to the wind environment or not acclimated, and three levels of gust intensity: 50, 100, and 200% (the scenarios' name are presented in Table 2). The outputs were the tree resistance values and the numbers of surviving trees every 100 time steps up to 2000 time steps. The ABM simulated each of these scenarios with 100 separate iteration based on Byrne (2013). The outputs of the simulations were assumed to be proportion data (always same start values). Using the 200 test outputs of all agents (trees, gusts and background-winds) from Scenario N-5m-100%, the average width of the confidence interval was 0.02 and the coefficient of variation (CV, standard deviation divided by sample mean) was 0.21 at 95% confidence level. Assuming variations of these values in the scenarios, we set the desired width of confidence interval to 0.05, so 99 was chosen as the minimum number of model runs with  $CV = 0.25$  in Byrne (2013). The first 100 time steps were used to make the number of gust agents stable; the damage starts occurring after 100 time steps. The output values from the 100-time runs were averaged based on steps and distances from the forest edge.

For analysing the outputs from the ABM, the tree data between 280 and 300 m ( $14$  and  $15 \times$  tree height) was first extracted. The gust and background-agents could not continuously move toward the outside of the simulation boundary, so some of the agents stayed at 300 m for a while. We then applied a balanced two-way analysis of variance (ANOVA) to find how the tree resistance mean values were affected by the distance from the forest edge (classified as the distance (280 m) in tree heights (20 m) up to  $14 \times$  tree height: 71 column variables) with time (classified for every 100 steps up to 2000 steps: 20 row variables). To make a balanced matrix of the two-way ANOVA, we used the first 71 simulation results from 100 simulation results. Analysis was conducted using R version 3.5.1 (the R Foundation for Statistical Computing) and MATLAB R2015b (Mathworks, Natick MA, USA).

ABM should be validated for use with the real-world problems and several validation methods are available based on the model purpose and characteristics (Grimm, 1999; Bert et al., 2014). On the other hand, especially the first attempts at modelling with ABM tend to be very simplified, so empirical validations using real data sets are often meaningless (Bert et al., 2011). In this paper, we created an ABM with highly artificial forest and environmental settings because such settings should reveal the fundamental model behaviour. Thus, we did not use specific validation methods in this paper, but discussed our results

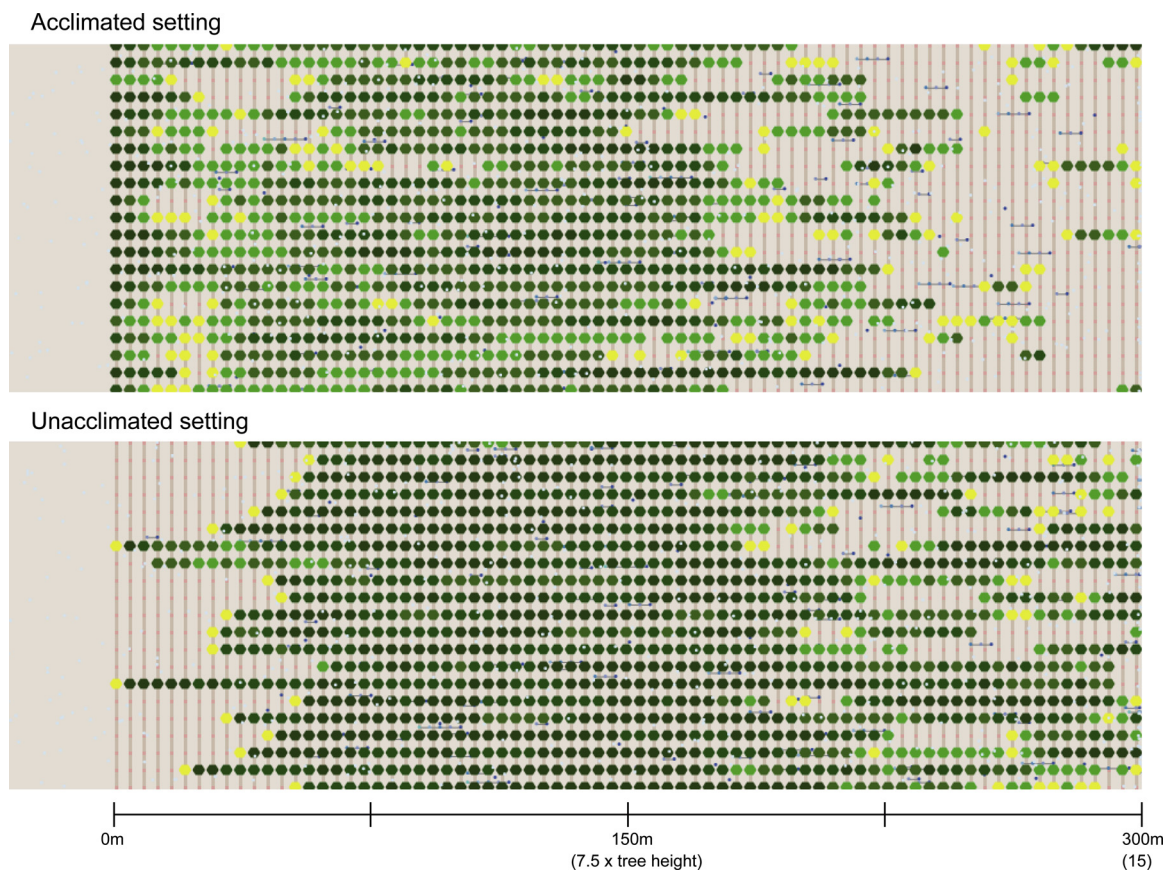


**Fig. 4.** Test simulations to demonstrate wind damage patterns of forests with  $4 \times 5$  m tree spacing and 100% gust intensity in the acclimated (1200 steps) and unacclimated (700 steps) settings. Green hexagon symbol indicates the tree agents. The resistance value decreases from darker to lighter green colours, and yellow colour indicated the resistance values  $< 100$ . The absence of a hexagon symbol means a damaged tree (For interpretation of the references to colour in this figure legend, the reader is referred to the web version of this article).

against known observations of the wind over forests and wind damage.

### 3. Results

#### 3.1. Testing the model

Fig. 4 presents the test results showing the tree resistance within the simulation boundaries (dark to light green, and yellow colours of the hexagonal symbols) with and without acclimation to the wind environment. No symbols on the lines indicate tree damage. The result with the acclimation indicated no damage to the edge trees but damage on the downwind trees around  $1 \times$  tree height and farther downwind at  $8 \times$  tree height. These damage patterns can be seen in Fig. 1(A) and (B), although the forest and environmental conditions are different. The simulation without the acclimation showed damage at the forest edge and damage propagation for 2 to  $3 \times$  tree height, and damage again farther downwind at  $10 \times$  tree height. The streamwise damage pattern back from the forest edge can be seen in Fig. 1(C). Since the actual scale and wind and tree characteristics of the photos in Fig. 1 are unknown, we could not directly compare our results with them, but at least the approximate damage patterns can be captured by the model.

For the simulations, we used a MacBookPro (MacOS Mojave version 10.14) with 2.8 GHz Intel Core i7 and 16GB 1600 MHz memory. The longest simulation was Scenario A-2m-50% (11 min/run) and the shortest N-7 m-200% (1.5 min/run).

#### 3.2. Simulations

The numbers of damaged trees with time were associated with the

tree spacing and gust intensities (Fig. 5). The trees without wind acclimation were more quickly damaged than those with acclimation at the beginning, but after 1000 time steps, the simulation with acclimated trees had more damage than those without acclimation in the 2 m tree spacing setting. The same situation was found with 50 and 100% gust intensities in the 5 m tree spacing setting after 1500 time steps and 100% gust intensity in the 7 m tree spacing setting after 1800 time steps.

Fig. 6 shows the speed of damage occurrence, which describes not only how many trees were damaged but also how trees were damaged. The trees without acclimation were damaged earlier due to the vulnerability of the edge trees (orange lines); in contrast, damage occurred slowly in the acclimated setting (blue lines) and became faster later. With 100% gust intensity, damage occurrence became faster in the acclimated setting with an increase in time, but the differences between the two settings became smaller with 200% gust intensity.

Tree resistance values varied with the distance from the forest edge and simulation time steps (Fig. 7). In the acclimated setting, the downwind trees next to the edge with 2 m tree spacing tended to lose their resistance values more quickly than at 5 and 7 m tree spacing, but the reduction got more moderate with an increase in distance from the edge. It led to larger resistance values between  $3 \times$  and  $10 \times$  tree height in the A-2m-100% than the other two acclimated scenarios. In the unacclimated setting, most of the edge trees were quickly damaged, in particular in the dense forest (N-2m-100%). Scenario N-7 m-100% also had reduced resistance values near to the forest edge, but the reduction was slower than in the dense forests. Larger resistance values were also found in the dense forest (N-2m-100%) than in the less dense forests. Between the acclimated and unacclimated settings, larger

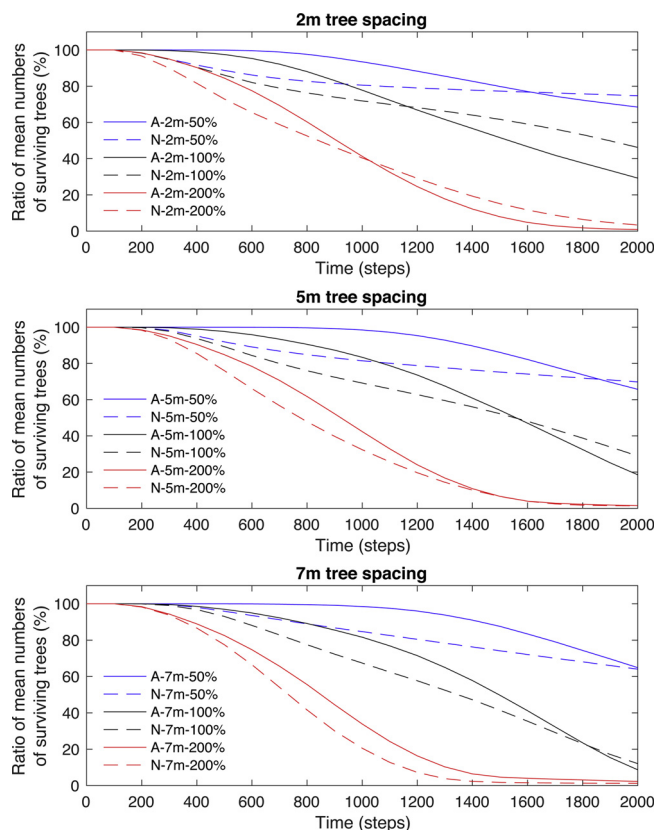


**Fig. 5.** Ratio of the numbers of surviving trees to the initial tree numbers against time steps based on the 2, 5, and 7 m of tree spacing and 50, 100, and 200% gust strength, with and without acclimation of the edge trees to the wind environment. The initial tree numbers are 2m: 3570 trees, 5m: 1470 trees, and 7 m: 1050 trees, existing between the forest edge and 280 m from the edge ( $14 \times$  tree height).

resistance values were found inside the forest without acclimation than with acclimation. This caused the two lines (acclimated and unacclimated) to converge and cross in Fig. 5.

Two-way ANOVA indicated three stages in the tree resistance values ( $p < 0.05$ ): constant, inconstant, and transition. The constant stage was found when the mean resistance values were significantly similar to the downwind mean resistance values for more than  $1 \times$  tree height; the inconstant stage (the most common stage) was when the mean resistance values were significantly different from the downwind mean resistance values for more than  $1 \times$  tree height; the transition stage had a gradual change in which only two neighboring mean values were significantly similar and such similar pairs were found for more than  $1 \times$  tree height (e.g. mean values between  $1.0$  and  $1.2 \times$  tree height were similar, but different between at  $1.0$  and  $1.4 \times$  tree height). These stages gave the details of how the damage changed with the distance from the edge during a simulation. We found the first constant stage between  $4.2$  and  $5.8 \times$  tree height from the forest edge in A-2m-100%,  $4.6$  and  $6.2 \times$  tree height in A-5m-100%,  $4.8$  and  $6.4 \times$  tree height in A-7m-100%,  $4.6$  and  $6.6 \times$  tree height in N-5m-100%,  $5.4$  and  $6.8 \times$  tree height in N-7m-100%. N-2m-100% had a mixed stage between  $4$  and  $7.2 \times$  tree height, which included the transition, constant, and again transition stage. The second constant stages occurred farther downwind at  $12.4 \times$  tree height in A-2m-100%,  $12 \times$  tree height in A-5m-100%,  $11.8 \times$  tree height in A-7m-100%, and  $13 \times$  tree height in both N-5m-100% and N-7m-100%. No second constant stage was found in N-2m-100%.

## 4. Discussion

This paper presents a new approach to modelling forest wind damage using a prototype ABM that simulated the dynamic process of damage in time and space. The current model was based on inductive methods together with our best understanding of gust and wind behaviour over forests, and changes in tree bending moment with distance from forest edges. In this section, we first discuss the estimated damage patterns created by the model. Second, the outcomes from the model are compared with empirical findings from previous studies. Finally, we identify possible improvements in the ABM for predicting wind damage in forests.

### 4.1. Testing the forest damage ABM

Wind damage in forests shows different spatial patterns associated with the forest condition and the duration of the damaging wind. We used the ABM technique to demonstrate damage with similar patterns (e.g. gap creations at the forest edge) to those observed in forests for both the acclimated and unacclimated settings (Figs. 1 and 4), despite using very simplified descriptions of gusts, background-wind, and tree resistance (Fig. 3). To make the model outputs closer to the observed damage, we would need to include detailed information on trees, forests, environment, and terrain in and outside forests. Forests, even homogeneous forests, never consist of exactly similar trees. Such differences lead to variations in tree damping and tree resistance due to competition with the neighbouring trees (Moore and Maguire, 2005; Hale et al., 2012; Schindler et al., 2012). Moreover, the environment outside a forest will lead to a change in airflow behaviour. If there are other forests in the windward direction with a gap to the subject forest, strong gusts will be created over the upwind forest, travel across the gap, and impact the damaged forest edge (Pöette et al., 2017). Other possible changes to improve the ABM will be discussed later.

### 4.2. Interpretation of the simulation results

We found different speeds of decrease in the average number of surviving trees with time, and the rates of decrease were reversed after a period between the acclimated and unacclimated settings, although the trees should be protected by the edge in the acclimated setting (Fig. 5). Fig. 6 shows a rapid decrease in the unacclimated setting earlier in the simulation and this is followed by a decrease in the surviving trees in the acclimated setting. This could be caused by the forest edge moving with associated changes in the gust and wind strength values. Near the forest edge in the unacclimated setting, the trees lost the tree resistance values quickly (Fig. 7), but later the forest edge moved inside, which brought stronger gusts further inside the forest. In contrast, strong gusts almost always stayed in the same position in the acclimated setting A-2m-100%, which resulted in more damage inside the simulation forest. The impacts from gusts could be farther inside the forest in the unacclimated setting, and might have been observable if there had been a longer simulation forest.

In the acclimated setting, the forest edge hardly moved; thus, the original forest edge affected more trees inside the forest during a simulation (Fig. 7). In A-2m-100% and A-5m-100%, the effects from the edge seemed to continue around  $9$  to  $10 \times$  tree height and became constant at  $12 \times$  tree height. These phenomena agree with the LES results of Dupont et al. (2011). Without acclimation, the edge effects were not so clear due to the rapid movement of the edge inside the forest. More rapid decrease in the resistance values near the edge in the A-2m-100% than A-7 m-100% would also reflect the finding from wind-tunnel experiments by Wuyts et al. (2008), in which the edge effect was found less deep into a dense forest.

The simulations with 100% gust intensity confirmed that the dynamic phenomena of damage (losing tree resistance due to gusts and the background wind) changed with time, so the storm duration time is

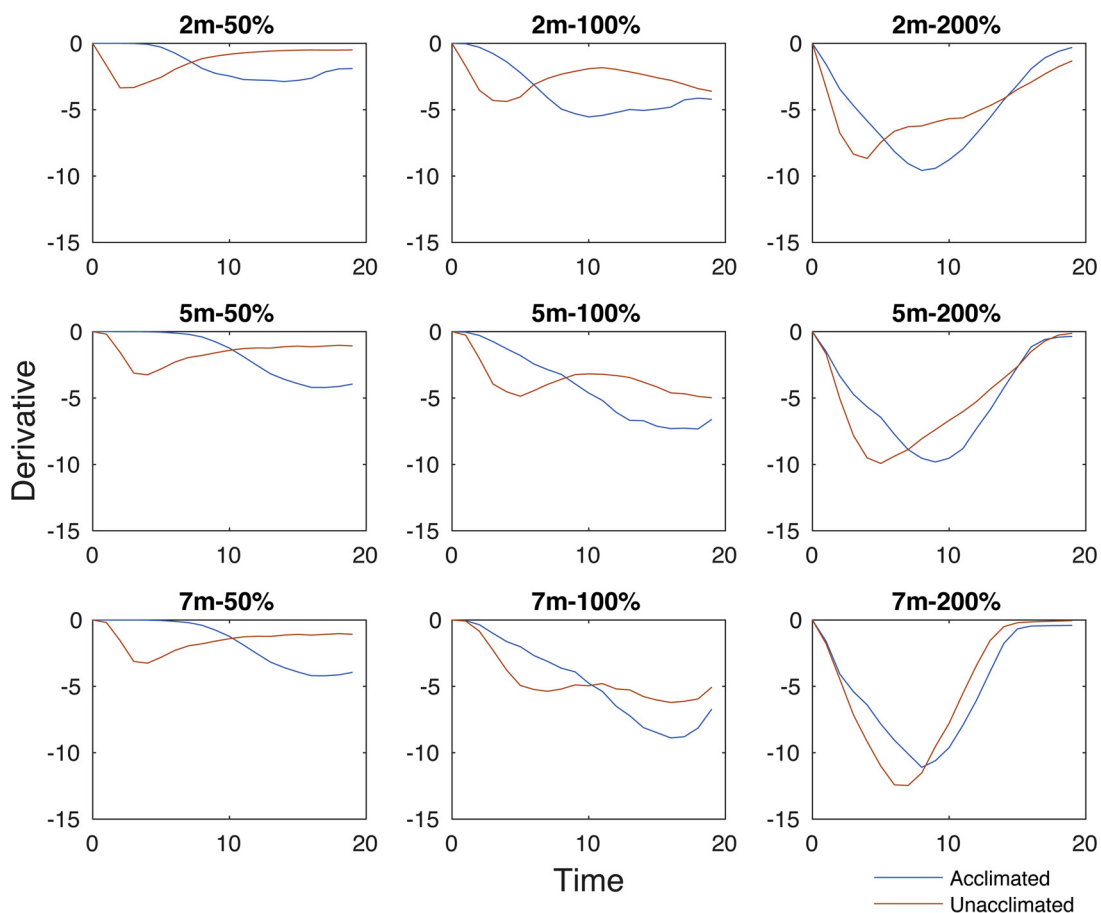


Fig. 6. Derivatives to show the rate of change in the number of surviving trees with time. Blue lines denote the derivatives of the acclimated setting and orange lines that of the unacclimated setting (For interpretation of the references to colour in this figure legend, the reader is referred to the web version of this article).

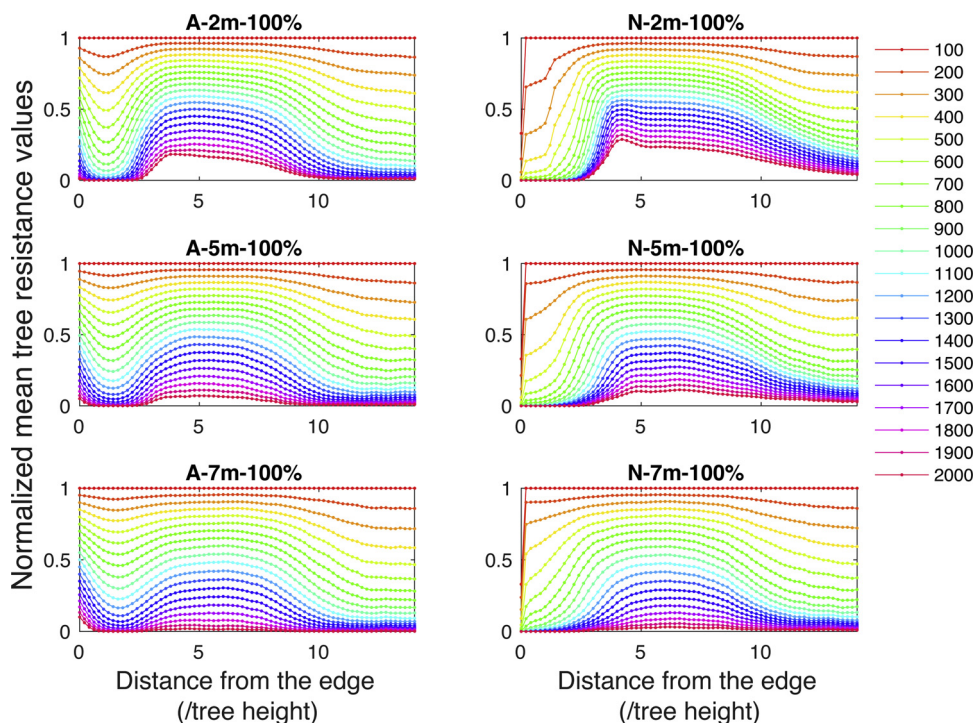


Fig. 7. Mean tree resistance values against distance from the forest edge with changing time steps in the acclimated and unacclimated settings including three tree spacings and 100% gust intensity. The values were normalized by the initial mean resistance values (at 0 step), denoted 1.

important in analysing wind damage. Three stages (constant, inconstant, and transition) helped to understand the wind damage process with changes in time and space. Although the experimental configurations were different from ours, Yang et al. (2006) found large standard deviation with a reducing wind moment between the edge and  $1.5 \times$  tree height and then it became more constant after  $8 \times$  tree height, indicating more constant pressure from winds (gusts) in their large eddy simulation. Although the ABM cannot reveal the direct mechanisms of developing damage stages, it can imitate the interaction between gusts and trees by integrating independent processes.

#### 4.3. Improving the current ABM

Adding more detailed characteristics to the tree, gust, and background-wind agents could improve the current ABM. The variability of tree vulnerability to wind is strongly associated with individual tree characteristics and stand structures, and could help improve model performance. For example, crown size is a key above-ground factor associated with wind damage occurrence including failure type (i.e., stem breakage or uprooting), with a smaller crown being associated with increasing tree damage (Dunham and Cameron, 2000), and crown size changes the frequency of tree sway (Moore and Maguire, 2005). More importantly, thinning alters tree vulnerability and increases wind loading due to the changes in tree characteristics including changes in crown size and the reduction in shelter from neighbouring trees (Cameron et al., 1995; Kamimura et al., 2017). Gusts are also more complex in time and space than what is represented in the ABM currently.

The formation of gust and background-wind agents needs to be changed depending on the simulation purpose. In this paper, we mainly focussed in the early conditions of vortex formation over a canopy (Finnigan et al., 2009) to find the damage patterns associated with a forest edge, which can be simulated in a two-dimensional configuration. If the detailed structure of the gusts and other scales of atmospheric motions need to be included, e.g. when considering a weather system and large scale forest damage, the simulations will have to be done in a three-dimensional configuration. The background-wind agents (an even simpler representation than the gust agents in this paper) should also vary in terms of their strength and total movement distance because these could be generated by large scale PBL eddies (Tischmacher and Ruck, 2013; Gromke and Ruck, 2018).

Spatial compositions such as gaps outside and inside the forest and tree spacing will also change the gust and background-wind agent behaviours. Tree damage forms new gaps of various size, which would alter the strength of wind (Pöette et al., 2017), and gust formation during a simulation might need to account for the newly created gaps inside forests in addition to the new forest edge. Tree spacing, related to canopy density, changes turbulent characteristics (Dupont and Brunet, 2008), but the current model does not account for the direct impacts of tree density on the gust and background-wind agent behaviour.

We simplified the environmental settings in this paper because such simple configurations allow the direct observation of the effect of the gusts and background-wind on forests. In the real world, however, there is a huge variety of environmental conditions that might be important in triggering damage, such as soil type and terrain conditions (topographic variation) (Moore, 2000). Including weather conditions, e.g., the duration time of strong winds during storms (Kamimura et al., 2013), would allow empirical validation of the ABM simulations based on observed damage data, and the model should produce more realistic damage patterns and intensities.

In spite of the possibilities of improving the ABM, we need to consider the trade-off between the complexity of agent representation and the time of simulation. In other words, time-consuming simulations reduce the advantages of the ABM approach. The results of the ABM in this paper showed that even simple parametrizations of gust, wind and trees could capture basic damage patterns and explain part of the

damage process. Using this approach has limitations, especially how to simplify the description of each agent and simulation environment without losing critical aspects of their natural variation. We used this modelling approach because of its simplicity and the benefits for forest managements of being able to test different forest configurations. With this purpose in mind, the best configurations and settings for the ABM approach need to be examined in a future study.

## 5. Conclusion

To develop a tool for decision making in forest management, we created a forest wind damage simulation model using an Agent-based modelling technique together with theories of gust, tree bending moment, and damage propagation within forests. The model consisted of gust, background (mean) wind, and tree agents, and was able to capture the patterns of damaged and undamaged trees after storms. In particular, it described damage propagation (gap creation) and changes in tree resistance within the simulation forest. Scenario studies were subsequently conducted in terms of trees acclimated and unacclimated to their local wind environment, differences in tree density, and three levels of gust strength. We found that the damage speeds between acclimated and unacclimated settings became smaller with an increase in the gust intensity; a decrease in tree density reduced the shelter effect of the forest; damage occurrence was classified into three stages with time and distance from the forest edge. Therefore, overall, the ABM captures the basic damage patterns and processes at forest edges, which could be a useful new tool in understanding wind damage in forests as a function of forest structure and management.

## Acknowledgement

We are grateful to Emma Hart and Kevin Sim at Edinburgh Napier University for giving us the idea of using the agent-based modelling approach for studying forest wind damage. We thank Céline Meredieu in INRA who provided us with information on maritime pine forest management in the Nouvelle-Aquitaine region, and Graeme Prest in Forest Enterprise Scotland and John Moore in SCION, New Zealand, who kindly allowed us to reproduce their photographs in Fig. 1. Finally we thank Ebba Dellwik, DTU, Denmark and two reviewers who gave us helpful comments and suggestions for improving this paper.

## References

- Bascuñán, A., Moore, J.R., Walker, J.C.F., 2006. Variations in the dynamic modulus of elasticity with proximity to the stand edge in radiata pine stands on the Canterbury Plains, New Zealand. *N. Z. J. For.* 51 (3), 4–8.
- Belcher, S.E., Harman, I.N., Finnigan, J.J., 2012. The wind in the willows: flows in forest canopies in complex terrain. *Annu. Rev. Fluid Mech.* 44, 479–504. <https://doi.org/10.1146/annurev-fluid-120710-101036>.
- Bert, F.E., Podestá, G.P., Rovere, S.L., Menéndez, A.N., North, N., Tatara, E., Laciana, C.E., Weber, E., Toranzo, F.R., 2011. An agent based model to simulate structural and land use changes in agricultural systems of the Argentine pampas. *Ecol. Modell.* 222, 3486–3499. <https://doi.org/10.1016/j.ecolmodel.2011.08.007>.
- Bert, F.E., Rovere, S.L., Macal, C.M., North, M.J., Podestá, G.P., 2014. Lessons from a comprehensive validation of an agent based-model: The experience of the Pampas Model of Argentinean agricultural systems. *Ecol. Modell.* 273, 284–298. <https://doi.org/10.1016/j.ecolmodel.2013.11.024>.
- Brüchert, F., Gardiner, B., 2006. The effect of wind exposure on the tree aerial architecture and biomechanics of sitka spruce (*Picea sitchensis*, Pinaceae). *Am. J. Bot.* 93 (10), 1512–1521.
- Byrne, M.D., 2013. How many times should a stochastic model be run? An approach based on confidence intervals. *Proceedings of the 12th International Conference on Cognitive Modeling 2013*, 445–450.
- Byrne, K.E., Mitchell, S.J., 2013. Testing of WindFIRM/ForestGALES BC: a hybrid-mechanistic model for predicting windthrow in partially harvested stands. *Forestry* 86, 185–199. <https://doi.org/10.1093/forestry/cps077>.
- Cameron, A.D., Dunham, R.A., Petty, J.A., 1995. The effects of heavy thinning on stem quality and timber properties of silver birch (*Betula pendula* Roth). *Forestry* 68 (3), 275–285.
- Cucchi, V., Bert, D., 2003. Wind-firmness in *Pinus pinaster* Ait. Stands in Southwest France: influence of stand density, fertilisation and breeding in two experimental stands damaged during the 1999 storm. *Ann. For. Sci.* 60, 209–226.

- Dunham, R.A., Cameron, A.D., 2000. Crown, stem and wood properties of winddamaged and undamaged Sitka spruce. *For. Ecol. Manage.* 135 (1–3), 73–81.
- Dupont, S., 2016. A simple wind-tree interaction model predicting the probability of wind damage at stand level. *Agric. For. Meteorol.* 224, 49–63. <https://doi.org/10.1016/j.agrformet.2016.04.014>.
- Dupont, S., Brunet, Y., 2008. Influence of foliar density profile on canopy flow: a large-eddy simulation study. *Agric. For. Meteorol.* 148, 976–990. <https://doi.org/10.1016/j.agrformet.2008.01.014>.
- Dupont, S., Brunet, Y., 2009. Coherent structures in canopy edge flow: a large-eddy simulation study. *J. Fluid Mech.* 630, 93–128. <https://doi.org/10.1017/S0022112009006739>.
- Dupont, S., Bonnefond, J., Irvine, M., Lamaud, E., Brunet, Y., 2011. Long-distance edge effects in a pine forest with a deep and sparse trunk space: in situ and numerical experiments. *Agric. For. Meteorol.* 151, 328–344. <https://doi.org/10.1016/j.agrformet.2010.11.007>.
- Dupont, S., Pivato, D., Brunet, Y., 2015. Wind damage propagation in forests. *Agric. For. Meteorol.* 214–215, 243–251. <https://doi.org/10.1016/j.agrformet.2015.07.010>.
- Finnigan, J.J., Brunet, Y., 1995. Turbulent airflow in forests on flat and hilly terrain. In: Coutts, M.P., Grace, J. (Eds.), *Wind and Trees*. Cambridge University Press, Cambridge, pp. 3–40.
- Finnigan, J.J., Shaw, R.H., 2000. A wind-tunnel study of airflow in waving wheat: an EOF analysis of the structure of the large-eddy motion. *Boundary-Layer Meteorol.* 96 (1), 211–255. <https://doi.org/10.1023/A:1002618621171>.
- Finnigan, J.J., Shaw, R.H., Patton, E.G., 2009. Turbulence structure above a vegetation canopy. *J. Fluid Mech.* 637, 387–424. <https://doi.org/10.1017/S0022112009990589>.
- Gardiner, B.A., 1994. Wind and wind forces in a plantation spruce forest. *Boundary-Layer Meteorol.* 67, 161–186. <https://doi.org/10.1007/BF00705512>.
- Gardiner, B.A., 1995. Wind tree interactions. In: Courts, M.P., Grace, J. (Eds.), *Wind and Trees*. Cambridge University Press, Cambridge, pp. 41–59.
- Gardiner, B.A., Stacey, G.R., Belcher, R.E., Wood, C.J., 1997. Field and wind tunnel assessments of the implications of respacing and thinning for tree stability. *Forestry* 70 (3), 233–252. <https://doi.org/10.1093/forestry/70.3.233>.
- Gardiner, B., Peltola, H., Kellomaki, S., 2000. Comparison of two models for predicting the critical wind speeds required to damage coniferous trees. *Ecol. Modell.* 129 (1), 1–23. [https://doi.org/10.1016/S0304-3800\(00\)00220-9](https://doi.org/10.1016/S0304-3800(00)00220-9).
- Gardiner, B., Marshall, B., Achim, A., Belcher, R., Wood, C., 2005. The stability of different silvicultural systems: a wind-tunnel investigation. *Forestry* 78 (5), 471–484.
- Gardiner, B., Berry, P., Moulia, B., 2016. Review: wind impacts on plant growth, mechanics and damage. *Plant Sci.* 245, 94–118. <https://doi.org/10.1016/j.plantsci.2016.01.006>.
- Garratt, J.R., 1990. The internal boundary layer - a review. *Boundary-layer Meteorol.* 47, 17–40.
- Grimm, V., 1999. Ten years of individual-based modelling in ecology: what have we learned and what could we learn in the future? *Ecol. Modell.* 115, 129–148.
- Grimm, V., Berger, U., Bastiansen, F., Eliassen, S., Ginot, V., Giske, J., Goss-Custard, J., Grand, T., Heinz, S.K., Huse, G., Huth, A., Jepsen, J.U., Jørgensen, C., Mooij, W.M., Müller, B., Pe'er, G., Piou, C., Railsback, S.F., Robbins, A.M., Robbins, M.M., Rossmanith, E., Rügen, N., Strand, E., Souissi, S., Stillman, R.A., Vabø, R., Visser, U., DeAngelis, D.L., 2006. A standard protocol for describing individual-based and agent-based models. *Ecol. Modell.* 198, 115–126. <https://doi.org/10.1016/j.ecolmodel.2006.04.023>.
- Gromke, C., Ruck, B., 2018. On wind forces in the forest-edge region during extreme-gust passages and their implications for damage patterns. *Boundary-Layer Meteorol.* <https://doi.org/10.1007/s10546-018-0348-4>. (published online 16 March 2018).
- Hale, S.E., Gardiner, B.A., Wellpott, A., Nicoll, B.C., Achim, A., 2012. Wind loading of trees: influence of tree size and competition. *Eur. J. For.* 131, 203–217. <https://doi.org/10.1007/s10342-010-0448-2>.
- Huston, M., DeAngelis, D., Post, W., 1988. New Models Unify Computer be explained by interactions among individual organisms. *Bioscience* 38 (10), 682–691.
- Kaimal, J., Finnigan, J.J., 1994. *Atmospheric boundary layer flows. Their Structure and Measurement*. Oxford University Press, Oxford.
- Kamimura, K., Saito, S., Kinoshita, H., Kitagawa, K., Uchida, T., Mizunaga, H., 2013. Analysis of wind damage caused by multiple tropical storm events in Japanese *Cryptomeria japonica* forests. *Forestry* 86, 411–420. <https://doi.org/10.1093/forestry/cpt011>.
- Kamimura, K., Gardiner, B.A., Koga, S., 2017. Observations and predictions of wind damage to *Larix kaempferi* trees following thinning at an early growth stage. *Forestry* 90 (4), 530–540. <https://doi.org/10.1093/forestry/cpx006>.
- Mitchell, S.J., 2013. Wind as a natural disturbance agent in forests: a synthesis. *Forestry* 86, 147–157. <https://doi.org/10.1093/forestry/cps058>.
- Moore, J.R., 2000. Differences in maximum resistive bending moments of *Pinus radiata* trees grown on a range of soil types. *For. Ecol. Manage.* 135 (1–3), 63–71.
- Moore, J.R., Maguire, D.A., 2005. Natural sway frequencies and damping ratios of trees: influence of crown structure. *Trees* 19, 363–373.
- Peltola, H., Kellomäki, S., Väisänen, H., Ilkonen, V.-P., 1999. A mechanistic model for assessing the risk of wind and snow damage to single trees and stands of Scots pine, Norway spruce, and birch. *Can. J. For. Res.* 29, 647–661.
- Pöette, C., Gardiner, B., Dupont, S., Harman, I., Böhm, M., Finnigan, J., Hughes, D., Brunet, Y., 2017. The impact of landscape fragmentation on atmospheric flow: a wind-tunnel study. *Boundary-Layer Meteorol.* 163 (3), 393–421. <https://doi.org/10.1007/s10546017-0238-1>.
- Railsback, S.F., Grimm, V., 2010. *Agent-Based and Individual-Based Modeling*. Princeton University Press, Princeton.
- Raupach, M.R., Finnigan, J.J., Brunet, Y., 1996. Coherent Eddies and Turbulence in Vegetation Canopies: the Mixing-Layer Analogy. pp. 351–382.
- Seidl, R., Rammer, W., Blennow, K., 2014. Simulating wind disturbance impacts on forest landscapes: tree-level heterogeneity matters. *Environ. Model. Softw.* 51, 1–11. <https://doi.org/10.1016/j.envsoft.2013.09.018>.
- Schindler, D., Fugmann, H., Schönborn, J., Mayer, H., 2012. Coherent response of a group plantation-grown Scots pine trees to wind loading. *Eur. J. For. Res.* 131 (1), 191–202. <https://doi.org/10.1007/s10342-010-0474-0>.
- Tischmacher, M., Ruck, B., 2013. Interaction of gusts and forest edges – an experimental wind-tunnel study. *Forestry* 86 (5), 523–532. <https://doi.org/10.1093/forestry/cpt029>.
- Wilensky, U., Rand, W., 2015. *An Introduction to Agent-Based Modeling*. The MIT Press, Cambridge.
- Wuyts, K., Verheyen, K., De Schrijver, A., Cornelis, W.M., Gabriels, D., 2008. The impact of forest edge structure on longitudinal patterns of deposition, wind speed, and turbulence. *Atmos. Environ.* 42 (37), 8651–8660. <https://doi.org/10.1016/j.atmosenv.2008.08.010>.
- Yang, B., Shaw, R.H., Paw, U.K.T., 2006. Wind loading on trees across a forest edge: a large eddy simulation. *Agric. For. Meteorol.* 141 (2–4), 133–146. <https://doi.org/10.1016/j.agrformet.2006.09.006>.